

Beyond Poisson-Boltzmann: Fluctuations and Correlations

Roland R. Netz[§] and Henri Orland*

[§]Max-Planck-Institut für Kolloid- und Grenzflächenforschung, Kantstr. 55, 14513 Teltow, Germany

*Service de Physique Théorique, CEA-Saclay, 91191 Gif sur Yvette, France

(February 1, 2008)

We formulate the non-linear field theory for a fluctuating counter-ion distribution in the presence of a fixed, arbitrary charge distribution. The Poisson-Boltzmann equation is obtained as the saddle-point, and the effects of fluctuations and correlations are included by a loop-wise expansion around this saddle point. We show that the Poisson equation is obeyed at each order in the loop expansion and explicitly give the expansion of the Gibbs potential up to two loops. We then apply our formalism to the case of an impenetrable, charged wall, and obtain the fluctuation corrections to the electrostatic potential and counter-ion density to one-loop order without further approximations. The relative importance of fluctuation corrections is controlled by a single parameter, which is proportional to the cube of the counter-ion valency and to the surface charge density. We also calculate effective interactions between charged particles, which reflect counter-ion correlation effects.

PACS. 82.70.-y - Disperse Systems.

PACS. 61.20.Qg - Associated Liquids.

PACS. 82.45.+z - Electrochemistry.

I. INTRODUCTION

The behavior of charged, fluctuating systems is an old problem in chemistry and physics and is of importance for very diverse disciplines. In this article we will be concerned with the distribution of counter ions around charged objects, which is experimentally realized whenever an object with dissociable surface groups is brought in contact with water (or some other high-dielectric solvent). In such a situation, the counter ions will be attracted to the oppositely charged object, but also repelled from other counter ions. The characteristic feature of charged systems is that the Coulomb interaction is long-ranged, which gives these systems very special properties. Since, in general, one counter ion interacts with many different counter ions simultaneously, the mean-field approach is very successful and can be used to describe experiments or simulations quantitatively. Exact solutions of the so-called Poisson Boltzmann equation, which determines the electrostatic potential distribution on a mean-field level, are available for planar [1–3] and cylindrical [4] geometries. A very readable introduction into the Poisson-Boltzmann (PB) approach is given in Ref. [5]. There are several factors which contribute to deviations from the PB equation, including additional, short-ranged interactions and solvent effects. In this article we will consider deviations due to *fluctuations and correlations*. These effects have been incorporated for the single charged wall by modified PB equations [6], by integral equation theories [7,8], and by numerical methods [9–12]. In general, one finds correlation effects to become important for ions of high valency, and packing effects dominate the ion distribution for very bulky ions or high ion concentration. For the case of counter ions or electrolyte solutions between two charged walls, there have been a number of studies using integral equations [13–15] and Monte-Carlo methods [16,17]. An exhaustive review has been given by Attard [18]. The main result of these studies is that correlations can lead to an effective attraction between similarly charged walls for high enough ion valency. There have been a few attempts of using field theoretic methods to go beyond mean-field theory for charged systems. Here we only mention the works by Podgornik and Zeks [19] and by Attard and coworkers [20], who expanded around the mean-field solution and calculated within additional approximations fluctuation corrections to the interaction between two charged, planar walls.

In this article we consider a system of mobile, point-like counter ions in the presence of a fixed charge distribution, and formulate the field-theoretic framework for going beyond the Poisson-Boltzmann description. As has been realized by many others before, the Poisson-Boltzmann equation constitutes the *saddle point* of the exact field theory. We first reformulate this theory by a loop-wise expansion around the saddle point. The Poisson equation, which relates the electrostatic potential to the counter ion distribution, is obeyed at each level of this loop expansion. Clearly, the counter-ions are not distributed according to the Boltzmann weight, and correlations and fluctuations lead to pronounced deviations from the Poisson-Boltzmann predictions. The description is considerably facilitated by a

Legendre transformation, after which we obtain the Gibbs potential as a function of a fixed electrostatic potential distribution. This transformation restricts the number of diagrams to so-called one-particle-irreducible diagrams. The electrostatic potential is given by the solution of the equation of state.

We then apply this general formalism to the case of counter ions confined to a half space and next to a charged wall. We calculate without further approximations the one-loop correction to the electrostatic potential distribution and the counter-ion distribution. Due to correlations the counter ions are more densely packed close to the wall than predicted by the PB solution. This is in accord with previous Monte-Carlo simulations and with the intuitive expectation, since mean field usually overestimates repulsive interactions due to the neglect of correlations. The relative importance of fluctuation corrections to the electrostatic potential is measured by the single parameter $q^3\sigma\ell_B^2$, where σ is the surface charge density of the planar surface, ℓ_B is the distance at which two elementary charges interact with thermal energy, and q denotes the counter-ion valency. Since the thickness of the counter ion distribution is, according to the mean-field prediction, given by $\mu \sim 1/(q\sigma\ell_B)$, the average counter-ion concentration follows as $c \sim \sigma/q\mu$ and our effective fluctuation parameter can be rewritten as $q^3\sigma\ell_B^2 \sim (q^2\ell_B c^{1/3})^{3/2}$ and thus measures the electrostatic interaction energy between two counter ions at their average separation (in units of the thermal energy); it is thus related to the plasma parameter. For vanishing values of $q^3\sigma\ell_B^2$ mean field theory becomes exact and fluctuation corrections are unimportant. On the other hand, since the counter ion valency comes in as a cubic power, it is clear that by going from monovalent to divalent ions, fluctuation effects become much more pronounced, in accord with experiments and simulations. Our results, which are obtained only to first order in the loop expansion, become unreliable for large values of $q^3\sigma\ell_B^2$. A clear break down of our expansion is indicated by an unphysical negative density of counter ions, which occurs at $q^3\sigma\ell_B^2 \simeq 12$.

In Section II we formulate the general field-theoretic description for an ensemble of fluctuating counter ions in the presence of a fixed charge distribution. The main steps consist of i) formulating the initial partition function as a field theory using a Hubbard-Stratonovich transformation, ii) going to the grand-canonical ensemble, iii) expanding the action around the saddle-point, and iv) performing another Legendre transformation after which the Gibbs potential depends on the electrostatic potential. In Section III we show how the electrostatic potential follows from the equation of state, and in Section IV we give explicit results for the case of a single charged wall. In Section V we calculate the effective interaction between charged test particles, and Section VI is devoted to a brief discussion.

II. NON-LINEAR FIELD THEORY FOR CHARGED SYSTEMS

The partition function for N mobile counter ions of valency q , interacting with an arbitrary fixed charge distribution, $\sigma(\mathbf{r})$, reads

$$Z_N = \frac{1}{N!} \left[\prod_{i=1}^N \int d\mathbf{r}_i \right] \exp \left\{ -q^2 \sum_{j>k} v(\mathbf{r}_j - \mathbf{r}_k) + q \int d\mathbf{r} \sigma(\mathbf{r}) \sum_j v(\mathbf{r} - \mathbf{r}_j) \right\}. \quad (1)$$

We assume the counter ions to be point-like particles, and only include the Coulomb interaction between ions, $v(\mathbf{r}) \equiv \ell_B/r$, where ℓ_B is the Bjerrum length defined as $\ell_B \equiv e^2/(4\pi\epsilon k_B T)$. We also neglect any image charge effects in the present formulation of our theory. The charge distribution $\sigma(\mathbf{r})$ in general also contains test particles, the presence of which allows to calculate the effective interaction between charges, as we will demonstrate in Section VI. Introducing the particle density operator

$$\hat{\rho}(\mathbf{r}) \equiv \sum_{i=1}^N \delta(\mathbf{r} - \mathbf{r}_i), \quad (2)$$

we can rewrite the partition function as

$$Z_N[h] = \frac{1}{N!} \left[\prod_{i=1}^N \int d\mathbf{r}_i \right] \exp \left\{ -\frac{1}{2} \int d\mathbf{r} d\mathbf{r}' [q\hat{\rho}(\mathbf{r}) - \sigma(\mathbf{r})] v(\mathbf{r} - \mathbf{r}') [q\hat{\rho}(\mathbf{r}') - \sigma(\mathbf{r}')] + \int d\mathbf{r} \hat{\rho}(\mathbf{r}) h(\mathbf{r}) \right\}. \quad (3)$$

There is no need to subtract the diagonal terms involving self interactions at this point, because they will be canceled by a one-point renormalization at a later stage. Using the generating field h , the average counter ion density can be calculated as

$$\langle \hat{\rho}(\mathbf{r}) \rangle = \frac{\delta Z_N[h]}{Z_N[h] \delta h(\mathbf{r})} \Big|_{h=0}. \quad (4)$$

Correlation functions can be calculated by taking multiple functional derivatives with respect to h . Noting that the operator-inverse of the Coulomb interaction is

$$v^{-1}(\mathbf{r}) = -\frac{\nabla^2 \delta(\mathbf{r})}{4\pi\ell_B},$$

the partition function is after a Hubbard-Stratonovich transformation given by

$$Z_N[h] = \frac{1}{N!} \int \frac{\mathcal{D}\phi}{Z_0} \exp \left\{ -\int d\mathbf{r} \left[\frac{1}{2\tilde{\ell}_B} (\nabla\phi)^2 + \frac{\imath\sigma(\mathbf{r})\phi(\mathbf{r})}{q} \right] \right\} \left[\int d\mathbf{r} e^{-\imath\phi(\mathbf{r})+h(\mathbf{r})} \right]^N, \quad (5)$$

where we introduced the rescaled Bjerrum length $\tilde{\ell}_B \equiv 4\pi q^2 \ell_B$. In the above expression, Z_0 denotes the partition function of the Coulomb operator, $Z_0 \sim \sqrt{\det v}$. Using the definition Eq. (4), the average particle density turns out to be

$$\langle \hat{\rho}(\mathbf{r}) \rangle = N \left\langle \frac{e^{-\imath\phi(\mathbf{r})}}{\int d\mathbf{r} e^{-\imath\phi(\mathbf{r})}} \right\rangle, \quad (6)$$

and the normalization property of the density distribution, $\int d\mathbf{r} \hat{\rho}(\mathbf{r}) = N$, is self-evident. The two-point cumulant correlation function (for $\mathbf{r} \neq \mathbf{r}'$) follows as

$$\begin{aligned} \langle \hat{\rho}(\mathbf{r}) \hat{\rho}(\mathbf{r}') \rangle &= \frac{\delta^2 Z_N[h]}{Z_N[h] \delta h(\mathbf{r}) \delta h(\mathbf{r}')} \Big|_{h=0} \\ &= N(N-1) \left\langle \frac{e^{-\imath\phi(\mathbf{r})-\imath\phi(\mathbf{r}')}}{\left[\int d\mathbf{r} e^{-\imath\phi(\mathbf{r})} \right]^2} \right\rangle, \end{aligned} \quad (7)$$

and higher-order correlation function can be calculated in a similar manner. The functional form of the particle distribution, Eq.(6), shows that $\imath\phi$ is the reduced electric potential. The partition function is brought into a more manageable form by going to the grand-canonical ensemble,

$$Z[\varrho, h] \equiv \sum_{N=0}^{\infty} \lambda^N Z_N[h] = \int \frac{\mathcal{D}\phi}{Z_0} \exp \left\{ -\ell \mathcal{H}[\phi, h] + \imath \ell \int d\mathbf{r} \phi(\mathbf{r}) \varrho(\mathbf{r}) \right\}. \quad (8)$$

where λ is the fugacity of the counter-ions, and the Hamiltonian is defined as

$$\mathcal{H}[\phi, h] \equiv \int d\mathbf{r} \left[\frac{1}{2\tilde{\ell}_B} (\nabla\phi)^2 + \frac{\imath\sigma(\mathbf{r})\phi(\mathbf{r})}{q} - \lambda e^{-\imath\phi(\mathbf{r})+h(\mathbf{r})} \right] \quad (9)$$

and we added a source term to the partition function in such a way that one can calculate directly the reduced electrostatic potential

$$\psi(\mathbf{r}) \equiv \langle \imath\phi(\mathbf{r}) \rangle = \frac{\delta \ln Z[\varrho, h]}{\ell \delta \varrho(\mathbf{r})}. \quad (10)$$

In the grand-canonical partition function, Eq.(8), we arbitrarily multiplied the action by a constant ℓ which plays the role similar to the inverse Planck's constant in front of the action integral in Quantum Field Theory. This constant serves as an expansion parameter in our systematic treatment of fluctuation effects and counts the number of diagrammatic loops. The fugacity λ is related to the total number of ions by

$$\lambda \frac{\partial \ln Z[\varrho, h]}{\ell \partial \lambda} = \langle N \rangle = \lambda \int d\mathbf{r} \langle e^{-\imath\phi(\mathbf{r})} \rangle \quad (11)$$

which establishes a useful relation between λ and N . The particle density is obtained from the grand-canonical partition function Eq.(8) using the definition Eq.(4) and reads

$$\langle \hat{\rho}(\mathbf{r}) \rangle = \lambda \langle e^{-\imath\phi(\mathbf{r})} \rangle.$$

Likewise, the two-point correlation function (for $\mathbf{r} \neq \mathbf{r}'$) reads

$$\langle \hat{\rho}(\mathbf{r}) \hat{\rho}(\mathbf{r}') \rangle = \lambda^2 \left\langle e^{-\imath\phi(\mathbf{r}) - \imath\phi(\mathbf{r}')} \right\rangle, \quad (12)$$

which is simpler than the canonical form, Eq.(7); higher-order correlation function can be calculated similarly. In the following we will be interested in calculating the Gibbs potential $\Gamma[\psi, h]$ which depends on the reduced electric potential $\psi(\mathbf{r})$; it is related to $\ln Z[\varrho, h]$ by a Legendre transform

$$\Gamma[\psi, h] + \ln Z[\varrho, h] = \ell \int d\mathbf{r} \psi(\mathbf{r}) \varrho(\mathbf{r}). \quad (13)$$

Using the definition (10) we obtain from the definition of the Legendre transform (13) the inverse relation

$$\varrho(\mathbf{r}) = \frac{\delta \Gamma[\psi, h]}{\ell \delta \psi(\mathbf{r})}. \quad (14)$$

We will perform the Legendre transformation using a loop expansion, using methods developed by Schwinger [21] and closely follow the notation of Brézin, Le Guillou, and Zinn-Justin [22]. To that end, we expand the Hamiltonian around a fixed value of the potential, the so-called classical field, denoted as $\psi_{\text{cl}}(\mathbf{r})$. At this point, we do not specify what this classical field is. We write

$$\phi(\mathbf{r}) = -\imath\psi_{\text{cl}}(\mathbf{r}) + \chi(\mathbf{r}) \quad (15)$$

and thus obtain the formal expansion

$$\mathcal{H}[\phi] - \imath \int d\mathbf{r} \phi(\mathbf{r}) \varrho(\mathbf{r}) = \mathcal{H}[-\imath\psi_{\text{cl}}] - \int d\mathbf{r} \varrho(\mathbf{r}) [\psi_{\text{cl}}(\mathbf{r}) + \imath\chi(\mathbf{r})] + \sum_{j=1} \frac{1}{j!} \int \mathcal{H}^{(j)}(\{\mathbf{r}_j\}; \psi_{\text{cl}}) \chi(\mathbf{r}_1) \cdots \chi(\mathbf{r}_j) d\mathbf{r}_1 \cdots d\mathbf{r}_j.$$

The vertex functions $\mathcal{H}^{(j)}$ are defined by

$$\mathcal{H}^{(j)}(\{\mathbf{r}_j\}; \psi_{\text{cl}}) \equiv \left. \frac{\delta^j \mathcal{H}[\phi]}{\delta \phi(\mathbf{r}_1) \cdots \delta \phi(\mathbf{r}_j)} \right|_{\phi = -\imath\psi_{\text{cl}}} \quad (16)$$

and of course depend on the function $\psi_{\text{cl}}(\mathbf{r})$ around which one expands. The function $\ln Z[\varrho]$ can now be evaluated by standard saddle-point methods, treating ℓ^{-1} as the expansion parameter. The saddle point $\psi_{\text{SP}}(\mathbf{r})$ is defined by

$$\left. \frac{\delta \mathcal{H}[\phi]}{\delta \phi(\mathbf{r})} - \imath \varrho(\mathbf{r}) \right|_{\phi = -\imath\psi_{\text{SP}}[\varrho]} = 0 \quad (17)$$

and depends on the source ϱ . Using the definition of the two-point propagator $G(\mathbf{r}, \mathbf{r}'; \psi_{\text{SP}})$,

$$\int d\mathbf{r} G(\mathbf{r}, \mathbf{r}'; \psi_{\text{SP}}) \mathcal{H}^{(2)}(\mathbf{r}, \mathbf{r}''; \psi_{\text{SP}}) = \delta(\mathbf{r}' - \mathbf{r}''),$$

we can diagrammatically expand the expression for $\ln Z[\varrho, h]$ and obtain up to two loops

$$\begin{aligned} \ln Z[\varrho, h] = \ell \int d\mathbf{r} \left\{ \frac{1}{2\ell_B} (\nabla \psi_{\text{SP}})^2 - \frac{\sigma(\mathbf{r}) \psi_{\text{SP}}(\mathbf{r})}{q} + \lambda e^{-\psi_{\text{SP}}(\mathbf{r}) + h(\mathbf{r})} + \varrho(\mathbf{r}) \psi_{\text{SP}}(\mathbf{r}) \right\} - \frac{1}{2} \ln \det \mathcal{H}^{(2)}[\psi_{\text{SP}}] \\ + \frac{1}{\ell} \left\{ -\frac{1}{8} \int d\mathbf{r}_1 \cdots d\mathbf{r}_4 \mathcal{H}^{(4)}(\{\mathbf{r}_4\}; \psi_{\text{SP}}) G(\mathbf{r}_1, \mathbf{r}_2; \psi_{\text{SP}}) G(\mathbf{r}_3, \mathbf{r}_4; \psi_{\text{SP}}) \right. \\ \left. + \int d\mathbf{r}_1 \cdots d\mathbf{r}_3 d\mathbf{r}'_1 \cdots d\mathbf{r}'_3 \mathcal{H}^{(3)}(\{\mathbf{r}_3\}; \psi_{\text{SP}}) \mathcal{H}^{(3)}(\{\mathbf{r}'_3\}; \psi_{\text{SP}}) \right. \\ \left. \left[\frac{1}{8} G(\mathbf{r}_1, \mathbf{r}_2; \psi_{\text{SP}}) G(\mathbf{r}'_1, \mathbf{r}'_2; \psi_{\text{SP}}) G(\mathbf{r}_3, \mathbf{r}'_3; \psi_{\text{SP}}) + \frac{1}{12} G(\mathbf{r}_1, \mathbf{r}'_1; \psi_{\text{SP}}) G(\mathbf{r}_2, \mathbf{r}'_2; \psi_{\text{SP}}) G(\mathbf{r}_3, \mathbf{r}'_3; \psi_{\text{SP}}) \right] \right\}. \quad (18) \end{aligned}$$

The one-loop diagram and the two-loop diagrams are schematically represented in Fig.1. In order to perform the Legendre transformation, we need the loop expansions for $\psi(\mathbf{r})$ and $\varrho(\mathbf{r})$, which are obtained from the definition (10) and the saddle-point equation (17), respectively. These expressions depend on the saddle-point potential ψ_{SP} . We

then have to expand all functions and vertices around the saddle point and reexpress the potential dependence as a function of the expectation value ψ . By inserting these expression into the Legendre transform, we obtain the loop expansion of the Gibbs potential,

$$\begin{aligned} \Gamma[\psi, h] = & -\ell \int d\mathbf{r} \left\{ \frac{1}{2\tilde{\ell}_B} (\nabla\psi)^2 - \frac{\sigma(\mathbf{r})\psi(\mathbf{r})}{q} + \lambda e^{-\psi(\mathbf{r})+h(\mathbf{r})} \right\} + \frac{1}{2} \ln \det \mathcal{H}^{(2)}[\psi] \\ & - \frac{1}{\ell} \left\{ -\frac{1}{8} \int d\mathbf{r}_1 \cdots d\mathbf{r}_4 \mathcal{H}^{(4)}(\{\mathbf{r}_4\}; \psi) G(\mathbf{r}_1, \mathbf{r}_2; \psi) G(\mathbf{r}_3, \mathbf{r}_4; \psi) \right. \\ & \quad \left. + \frac{1}{12} \int d\mathbf{r}_1 \cdots d\mathbf{r}_3 d\mathbf{r}'_1 \cdots d\mathbf{r}'_3 \mathcal{H}^{(3)}(\{\mathbf{r}_3\}; \psi) \mathcal{H}^{(3)}(\{\mathbf{r}'_3\}; \psi) \right. \\ & \quad \left. G(\mathbf{r}_1, \mathbf{r}'_1; \psi) G(\mathbf{r}_2, \mathbf{r}'_2; \psi) G(\mathbf{r}_3, \mathbf{r}'_3; \psi) \right\} \end{aligned} \quad (19)$$

The effect of the Legendre transformation is to cancel all one-particle-reducible diagrams, as expected. For the present case, the two-loop diagram to the right in Fig.1 is removed from the expansion.

III. THE EQUATION OF STATE

The equation of state is defined as

$$\frac{\delta\Gamma[\psi]}{\delta\psi(\mathbf{r})} = 0 \quad (20)$$

and completely determines the electrostatic potential. In the following, we will restrict ourselves to the one-loop order. Using the explicit form of the two-point vertex function, which follows from the definitions Eq.(9) and Eq.(16),

$$\mathcal{H}^{(2)}[\mathbf{r}, \mathbf{r}'; \psi] = \left(-\frac{\nabla^2}{\tilde{\ell}_B} + \lambda e^{-\psi(\mathbf{r})} \right) \delta(\mathbf{r} - \mathbf{r}'), \quad (21)$$

the equation of state can be explicitly written as

$$-\lambda e^{-\psi(\mathbf{r})} - \frac{\sigma(\mathbf{r})}{q} - \frac{\nabla^2 \psi(\mathbf{r})}{\tilde{\ell}_B} + \frac{\lambda}{2\ell} e^{-\psi(\mathbf{r})} G(\mathbf{r}, \mathbf{r}) = 0. \quad (22)$$

Note that from now on, we suppress the dependence of the two-point correlation function $G(\mathbf{r}, \mathbf{r}')$ on the electrostatic potential distribution ψ . The correlation function is determined by the equation

$$\left(-\frac{\nabla^2}{\tilde{\ell}_B} + \lambda e^{-\psi(\mathbf{r})} \right) G(\mathbf{r}, \mathbf{r}') = \delta(\mathbf{r} - \mathbf{r}'). \quad (23)$$

Finally, the number of mobile ions can be calculated according to Eq.(11) and is given by

$$\langle N \rangle = \lambda \int d\mathbf{r} e^{-\psi(\mathbf{r})} - \frac{\lambda}{2\ell} \int d\mathbf{r} e^{-\psi(\mathbf{r})} G(\mathbf{r}, \mathbf{r}). \quad (24)$$

The equation of state can be solved by a systematic expansion of all quantities which are to be determined in inverse powers of the loop parameter ℓ . At the one-loop order, only the leading term of G contributes and therefore an expansion of G itself is unnecessary. The electric potential and the fugacity have to be expanded to the next-leading order,

$$\psi(\mathbf{r}) = \psi_0(\mathbf{r}) + \ell^{-1} \psi_1(\mathbf{r}), \quad (25)$$

$$\lambda = \lambda_0 + \ell^{-1} \lambda_1. \quad (26)$$

The equation of state splits into two separate equations, the zero-loop equation

$$-\lambda_0 e^{-\psi_0(\mathbf{r})} - \frac{\sigma(\mathbf{r})}{q} - \frac{\nabla^2 \psi_0(\mathbf{r})}{\tilde{\ell}_B} = 0, \quad (27)$$

which is the ordinary Poisson Boltzmann equation, and the next-leading correction,

$$-\lambda_1 e^{-\psi_0(\mathbf{r})} + \lambda_0 e^{-\psi_0(\mathbf{r})} \psi_1(\mathbf{r}) - \frac{\nabla^2 \psi_1(\mathbf{r})}{\tilde{\ell}_B} + \frac{\lambda_0}{2} e^{-\psi_0(\mathbf{r})} G(\mathbf{r}, \mathbf{r}) = 0. \quad (28)$$

The correlation function is determined by

$$\left(-\frac{\nabla^2}{\tilde{\ell}_B} + \lambda_0 e^{-\psi_0(\mathbf{r})} \right) G(\mathbf{r}, \mathbf{r}') = \delta(\mathbf{r} - \mathbf{r}'). \quad (29)$$

The fugacity is at the zero-loop level determined by

$$\lambda_0 = \frac{\langle N \rangle}{\int d\mathbf{r} e^{-\psi_0(\mathbf{r})}} \quad (30)$$

and at the next-leading level by

$$\lambda_1 = \lambda_0 \frac{\int d\mathbf{r} e^{-\psi_0(\mathbf{r})} \psi_1(\mathbf{r})}{\int d\mathbf{r} e^{-\psi_0(\mathbf{r})}} + \frac{\lambda_0}{2} \frac{\int d\mathbf{r} e^{-\psi_0(\mathbf{r})} G(\mathbf{r}, \mathbf{r})}{\int d\mathbf{r} e^{-\psi_0(\mathbf{r})}}. \quad (31)$$

Combining the equations for ψ_1 and G , Eqs.(28) and (29), we obtain for the correction to the electrostatic potential

$$\psi_1(\mathbf{r}) = -\frac{\lambda_0}{2} \int d\mathbf{r}' e^{-\psi_0(\mathbf{r}')} G(\mathbf{r}', \mathbf{r}) \left[G(\mathbf{r}', \mathbf{r}') - \frac{2\lambda_1}{\lambda_0} \right], \quad (32)$$

which contains an implicit dependence on ψ_1 on the right-hand side through the dependence of λ_1 on ψ_1 , see Eq.(31). Algebraically solving Eqs.(31) and (32) we obtain

$$\int d\mathbf{r} e^{-\psi_0(\mathbf{r})} \psi_1(\mathbf{r}) = \frac{-(\lambda_0/2) \int d\mathbf{r} d\mathbf{r}' e^{-\psi_0(\mathbf{r}) - \psi_0(\mathbf{r}')} G(\mathbf{r}', \mathbf{r}) [G(\mathbf{r}, \mathbf{r}) - Z/Y]}{1 - (\lambda_0/Y) \int d\mathbf{r} d\mathbf{r}' e^{-\psi_0(\mathbf{r}) - \psi_0(\mathbf{r}')} G(\mathbf{r}', \mathbf{r})}, \quad (33)$$

where we used the short-hand notations

$$Y = \int d\mathbf{r} e^{-\psi_0(\mathbf{r})} \quad (34)$$

and

$$Z = \int d\mathbf{r} e^{-\psi_0(\mathbf{r})} G(\mathbf{r}, \mathbf{r}). \quad (35)$$

The one-loop correction to the electrostatic potential is therefore determined by Eq.(32) in conjunction with the equations determining G and λ_1 , Eqs.(29) and (31).

IV. SINGLE CHARGED IMPENETRABLE WALL

In the following we consider the case of a charged wall which is impenetrable for the counterions. The fixed charge distribution is given by $\sigma(\mathbf{r}) = \sigma \delta(z)$ where σ is the surface charge density at the charged wall. The solution for the one-dimensional Poisson-Boltzmann equation, Eq.(27), is

$$\psi_0(z) = 2 \ln(1 + z/\mu), \quad (36)$$

where $\mu = \sqrt{2/\tilde{\ell}_B \lambda_0} = 1/\sqrt{2\pi q^2 \ell_B \lambda_0}$ is the Gouy-Chapman length. Enforcement of the normalization condition, Eq.(30), leads to a relation between the surface charge density σ and the Gouy-Chapman length, $\sigma = q\lambda_0\mu$, which can be further transformed to $\lambda_0 = 2\pi\ell_B\sigma^2$ and $1/\mu = 2\pi\ell_B q\sigma$, the standard results.

A. Calculation of the correlation function

Due to lateral invariance, the Green's function $G(\mathbf{r}, \mathbf{r}')$ can be Fourier transformed in the directions perpendicular to the surface; the equation for the Green's function, Eq.(29), becomes

$$\left(-\frac{d^2}{dz^2} + p^2 + \tilde{\ell}_B \lambda_0 e^{-\psi_0(z)}\right) G(z, z', p) = \tilde{\ell}_B \delta(z - z'). \quad (37)$$

where \vec{p} are the Fourier variables in the lateral directions, and $p = |\vec{p}|$. The potential $\psi_0(z)$ is given by Eq.(36) for $z > 0$. Since the ions cannot penetrate into the wall, the counter-ion density is zero for $z < 0$, or, equivalently, we put $\psi_0(z) = \infty$ for $z < 0$. The solution can be obtained in a straightforward manner and reads

$$G(z, z', p) = \frac{\tilde{\ell}_B}{2p^5} \left(\frac{p}{z' + \mu} + p^2\right) \left[\left(-\frac{p}{z + \mu} + p^2\right) e^{p(z-z')} + \left(\frac{\frac{p}{z + \mu} + p^2}{1 + 2p^2\mu^2 + 2p\mu}\right) e^{-p(z+z')} \right] \quad (38)$$

for $z' > z > 0$. The solution for $z > z' > 0$ follows from Eq.(38) by an interchange of the arguments z and z' . In the limit $p = 0$ we obtain

$$G(z, z', p = 0) = \frac{\tilde{\ell}_B \mu (2 + (1 + z/\mu)^3)}{3(1 + z/\mu)(1 + z'/\mu)} \quad (39)$$

for $z' > z > 0$ (and with the coordinates interchanged for $z > z' > 0$). The self interaction is defined as the equal-point Green's function and follows from the partially Fourier-transformed Green's function as

$$G_{\text{self}}(z) = \int \frac{d^2 p}{(2\pi)^2} G(z, z, p). \quad (40)$$

The integral to be solved is, subtracting the (infinite) Coulomb self energy $G_{\text{self}}(z = \infty)$,

$$G_{\text{self}}(z) = \frac{\tilde{\ell}_B}{2} \int_0^\infty \frac{dp}{2\pi} \left[-\frac{1}{(z + \mu)^2 p^2} + \frac{1 + 2p^{-1}(z + \mu)^{-1} + p^{-2}(z + \mu)^{-2}}{1 + 2p^2\mu^2 + 2p\mu} e^{-2pz} \right]. \quad (41)$$

The integral can be performed by some intermediate transformations, and the result can be written in a scaling form as

$$G_{\text{self}}(z) = \frac{\tilde{\ell}_B}{4\pi\mu} g(z/\mu) \quad (42)$$

where the scaling function $g(x)$ is explicitly given by

$$g(x) = \frac{1}{2(1+x)^2} \left[i e^{(1-i)x} E_1[(1-i)x](1+ix)^2 - i e^{(1+i)x} E_1[(1+i)x](1-ix)^2 - 4x \right] \quad (43)$$

and plotted in Fig.2. The function $E_1[x]$ is the exponential-integral function [23]. The prefactor of the scaling function in Eq.(42),

$$\frac{\tilde{\ell}_B}{4\pi\mu} = \frac{q^2 \ell_B}{\mu} = 2\pi q^3 \ell_B^2 \sigma, \quad (44)$$

is a measure of the importance of correlation effects and thus the departure from mean-field behavior. We note that it is this single parameter combination which measures the relative importance of fluctuation corrections. Clearly, the cubic dependence on the counter-ion valency shows that fluctuation effects will become much more dominant for multivalent ions. As can be seen from Fig.2, the self energy is negative, which reflects the fact that the screening due to counter ions lowers the local free energy of charged particles. The scaling function $g(z/\mu)$ shows a minimum at a finite distance from the wall, $z/\mu \approx 0.2$. This maximum in screening is closely connected with a maximum in the counter-ion density at about this distance from the wall, as we will show in Section IV.C. The asymptotic behavior for small separations from the wall is

$$g(x) \simeq -\frac{\pi}{4} (1 - x \ln x) \quad (45)$$

and

$$g(x) \simeq -\frac{3}{2x} \quad (46)$$

for large separations. The functions Eqs.(45) and (46) are shown in Figs.2a and 2b as broken lines.

B. Calculation of the one-loop correction to the electrostatic potential

The solution of the equation for ψ_1 is considerably simplified by the fact that, for the specific mean-field potential given in Eq.(36), we find

$$\int dz G(z, z', p=0)e^{-\psi_0(z)} = \tilde{\ell}_B \mu^2 / 2 \quad (47)$$

independent of z' . It immediately follows from Eq.(32) that the integral $\int dz e^{-\psi_0(z)} \psi_1(z)$ is zero and, as a consequence, the equation for ψ_1 , Eq.(32), is independent of any constant appearing in the correlation function G . This holds in particular for the Coulombic self energy and therefore justifies that we neglected this (infinite) constant in the calculation of the self interaction. This is an example of a renormalization of a one-point correlation function, which otherwise is plagued by the (infinite) Coulombic self-energy. The normalization of the bare potential ψ_0 , Eq.(36) is

$$\int dz e^{-\psi_0(z)} = \mu. \quad (48)$$

The renormalization constant appearing in Eq.(32) thus is

$$\frac{2\lambda_1}{\lambda_0} = \frac{\int dz e^{-\psi_0(z)} G_{\text{self}}(z)}{\int dz e^{-\psi_0(z)}} = -\frac{\tilde{\ell}_B c_1}{4\pi\mu} \quad (49)$$

where the numerical constant is $c_1 = \int_0^\infty dx g(x)(1+x)^{-2} = 0.6208593$. Our final result for the potential is, according to Eq.(32),

$$\psi_1(z) = \frac{\tilde{\ell}_B}{4\pi\mu} \left[f(z/\mu) - \frac{c_1}{2} \right], \quad (50)$$

where the scaling function $f(x)$ is defined by

$$f(x) = - \int_0^x dx' \frac{2 + (1+x')^3}{3(1+x)(1+x')^3} g(x') - \int_x^\infty dx' \frac{2 + (1+x)^3}{3(1+x)(1+x')^3} g(x') \quad (51)$$

and graphically presented in Fig.3. The asymptotic behavior for small separations is

$$f(x) \simeq \frac{\pi}{8} \left(1 - \frac{x^3 \ln x}{3} \right) \quad (52)$$

and for large separations we obtain

$$f(x) \simeq \frac{\ln x}{2x}. \quad (53)$$

The asymptotic formulas are shown in Fig.3 as broken lines.

C. Calculation of the counter-ion density

The counter ion density $\rho(\mathbf{r})$ can be calculated from the Gibbs potential Eq.(19) by taking a derivative with respect to the generating field h . The result is, including the one-loop correction, given by

$$\rho(\mathbf{r}) = \lambda e^{-\psi(\mathbf{r})} - \frac{\lambda}{2\ell} e^{-\psi(\mathbf{r})} G(\mathbf{r}, \mathbf{r}) \quad (54)$$

and leads via integration to the total ion number N , Eq.(24), as it should. Subtracting the equation of state, Eq.(22), we obtain the Poisson equation,

$$\rho(\mathbf{r}) = -\frac{\sigma(\mathbf{r})}{q} - \frac{\nabla^2 \psi(\mathbf{r})}{\ell_B}. \quad (55)$$

In fact, the equation Eq.(55) is exact to all orders in the loop expansion, since the equation of state contains exactly the same terms as does the particle density and thus leads to an exact cancelation of all higher-loop terms. This is so because in the Hamiltonian Eq.(9), the generating field h enters in the same way as the fluctuating potential ϕ , except for the linear and quadratic terms. Expanding the counter ion density in powers of the loop parameter,

$$\rho(\mathbf{r}) = \rho_0(\mathbf{r}) + \ell^{-1}\rho_1(\mathbf{r}), \quad (56)$$

and using the loop-wise expansions of the fugacity λ and the electrostatic potential $\psi(\mathbf{r})$ introduced in Section III, the zero-loop (or mean-field) result for the counter ion density is

$$\rho_0(\mathbf{r}) = \lambda_0 e^{-\psi_0(\mathbf{r})} \quad (57)$$

and the one-loop correction reads

$$\rho_1(\mathbf{r}) = \lambda_0 e^{-\psi_0(\mathbf{r})} \left(\frac{\lambda_1}{\lambda_0} - \psi_1(\mathbf{r}) - \frac{1}{2}G(\mathbf{r}, \mathbf{r}) \right). \quad (58)$$

Using the explicit solution for the single charged wall, Eq.(36), and the result for the mean-field fugacity, $\lambda_0 = 2/\tilde{\ell}_B\mu^2$, the zero-loop density can be written as

$$\rho_0(z) = \left(\frac{2}{\tilde{\ell}_B\mu^2} \right) \frac{1}{(1+z/\mu)^2} \quad (59)$$

and the one-loop correction reads

$$\rho_1(z) = \left(\frac{2}{\tilde{\ell}_B\mu^2} \right) \frac{\tilde{\ell}_B}{4\pi\mu} h(z/\mu) \quad (60)$$

where the scaling function $h(x)$ can be written in terms of the previously defined scaling functions and reads

$$h(x) = -\frac{f(x) + g(x)/2}{(1+x)^2}. \quad (61)$$

In Fig.4 we plot the scaling function $h(x)$. The density correction vanishes at the charged wall, and for small separations the asymptotic behavior follows from Eqs. (45) and (52) as

$$h(x) \simeq -\frac{\pi}{8}x \ln x. \quad (62)$$

The density corrections is positive for $x < 1$, i.e. for distances from the wall smaller than the Gouy-Chapman length μ fluctuations and correlations lead to an enhanced density, quite in accord with expectations: Each counter ion is surrounded by a correlation hole, which is neglected on a mean-field level. Mean field theory therefore overestimates the repulsion between counter ions, and therefore underestimates the density close to the charged wall. This is in qualitative agreement with Monte-Carlo simulations [16]. We note that since the slope of the density correction is infinite close to the wall, see Eq.(62), our results predict always an initial increase of the counter-ion density as one moves away from the substrate. The total integral over the density correction vanishes; the increase in density close to the wall is therefore compensated by a decrease in density further away from the wall, as shown in Fig.4b. For large separations from the wall, the asymptotic behavior follows from Eqs. (45) and (52) as

$$h(x) \simeq -\frac{\ln x}{x^3}. \quad (63)$$

In Fig. 5 we plot the rescaled density $\bar{\rho}(z) = (\tilde{\ell}_B\mu^2/2)\rho(z)$ as a function of the rescaled distance from the wall z/μ , for four different values of the parameter $\tilde{\ell}_B/4\pi\mu$. The broken line, for $\tilde{\ell}_B/4\pi\mu = 0$, denotes the PB result, the other three solid lines are for $\tilde{\ell}_B/4\pi\mu = 1, 5, \text{ and } 10$, with the difference to the broken line increasing as the parameter $\tilde{\ell}_B/4\pi\mu$ increases. We see that already for rather small values of $\tilde{\ell}_B/4\pi\mu$, the one-loop result for the counter ion distribution is quite different from the PB result. The density depression far away from the wall is proportional to the parameter $\tilde{\ell}_B/4\pi\mu$. It is clear that for very large values of this parameter, the sum of the zero-loop and the one-loop densities will become negative. This in fact happens at $\tilde{\ell}_B/4\pi\mu \approx 12$, which clearly sets an upper limit to the applicability of the present one-loop calculation. It is likely that the one-loop calculation becomes quantitatively inaccurate even for smaller values of this parameter, but the precise value of $\tilde{\ell}_B/4\pi\mu$ when this happens can only be judged by a numerical calculation (such as Monte Carlo) or by a higher-loop calculation.

V. INTERACTION BETWEEN CHARGED PARTICLES

In this section we calculate the effective interaction between charged test particles. As mentioned before, test particles can be incorporated into the model by adding them to the charge distribution in Eq.(1) according to

$$\sigma(\mathbf{r}) \rightarrow \sigma(\mathbf{r}) + \sum_{j=1}^M Q_j \delta(\mathbf{r} - \mathbf{R}_j), \quad (64)$$

where we have considered a collection of $j = 1, \dots, M$ test particles with charges Q_j and positions \mathbf{R}_j . Inserting this shifted charge distribution into the grand-canonical partition function Eq. (8), the reduced test-particle free energy turns out to be

$$f(\{\mathbf{R}_M\}) = -\ln \left\langle e^{-\nu \sum_j Q_j \phi(\mathbf{R}_j)/q} \right\rangle. \quad (65)$$

Using the separation of the fluctuating field ϕ into the expectation value ψ and the fluctuations around the expectation value, Eq.(15), the free energy can be reexpressed as

$$f(\{\mathbf{R}_M\}) = \sum_{j=1}^M Q_j \psi(\mathbf{R}_j)/q + \frac{1}{2} \sum_{j,k=1}^M Q_j Q_k G(\mathbf{R}_j, \mathbf{R}_k)/q^2. \quad (66)$$

Using the loop-expansion of the electrostatic potential, ψ , Eq.(25), and the definition of the self interaction, G_{self} , Eq.(40), the free energy becomes on the one-loop level

$$f(\{\mathbf{R}_M\}) = \sum_{j=1}^M \left\{ \frac{Q_j}{q} [\psi_0(Z_j) + \psi_1(Z_j)] + \frac{Q_j^2}{2q^2} G_{\text{self}}(Z_j) \right\} + \sum_{j<k}^M \frac{Q_j Q_k}{q^2} G(\mathbf{R}_j, \mathbf{R}_k) \quad (67)$$

and thus separates into a single-particle part and a two-particle part. The single-particle contribution contains the ordinary Gouy-Chapman potential, $\psi_0(z)$, given by Eq.(36), a contribution due to fluctuation-induced changes of the electrostatic potential, $\psi_1(z)$, given by Eq.(50), and a contribution due to correlations between counterions and a test particle, $Q_j^2 G_{\text{self}}(z)$, given by Eq.(42). Since the correlation contribution is attractive and proportional to the square of the test-particle charge, it will be dominant for large test-particle charge and lead to attraction even in the case of a similarly charged wall. This somewhat surprising behavior has in fact been seen in Monte-Carlo simulations [11]. We note that on the two-loop level, in addition a three-point interaction appears.

Finally we will present results for the interaction between two particles in the neighborhood of the charged wall and thus under the influence of the loosely bound counter-ion cloud. To make the results somewhat more transparent, we will confine ourselves to particles which have the same vertical distance from the wall. The effective interaction then follows by Fourier transformation and reads

$$G(z, r) = \int \frac{dpp}{2\pi} G(z, z, p) \mathcal{J}_0(pr) \quad (68)$$

where the Green's function $G(z, z, p)$ is determined by Eq.(38) and $\mathcal{J}_0(x)$ denotes the Bessel function of the first kind [23]. For particles which are very close to each other, $r < \mu$, and/or very far apart from the charged surface, $z > r$, the interaction is basically unscreened and given by

$$G(z, r) \simeq \ell_B q^2 / r. \quad (69)$$

For particles that are far apart from each other, $r > \mu$, but close to the surface, $z < \mu$, the effective interaction is given by

$$G(z, r) \simeq \frac{2\ell_B q^2 \mu^2}{r^3} \left(1 - 4\frac{z}{\mu} + 6\frac{z^2}{\mu^2} + \dots \right). \quad (70)$$

The main feature is that the effective interaction is screened and thus reduced compared to the bare Coulomb interaction, but the screening is much weaker than for example in a salt solution and the interaction decays as an inverse cube of the distance. This behavior has previously been predicted by liquid-state calculations and is

interpreted as the effective dipole-dipole interaction between the test-charges and their associated counter-ion clouds [24–26]. The effective interaction between two induced dipoles is unscreened because the lower half-space is assumed to be impenetrable to ions and thus allows the unattenuated passage of electric field lines. From Eq.(70) it follows that the screening is maximal at a finite distance away from the wall. This is connected with the maximum in the counter-ion distribution, see Fig.4. For particles that are far apart from each other, $r > \mu$, and also relatively far apart from the surface, $\mu < z < r$, the effective interaction is given by

$$G(z, r) \simeq \frac{2\ell_B q^2 z^2}{r^3} \quad (71)$$

and thus increases gradually as one moves away from the surface. At a separation from the surface which equals the interparticle distance, $z \sim r$, the effective interaction has the same magnitude as the bare Coulomb interaction, and we find the effective interaction to cross over smoothly to the bare interaction as given by Eq.(69).

VI. DISCUSSION

In this article we have formulated the non-linear field theory for mobile counter ions under the influence of fixed charge distributions. We showed explicitly that the Poisson-Boltzmann equation corresponds to the saddle-point equation, and how correlations and fluctuations can be accounted for by a loop-wise expansion of the action around this saddle point. We find the Poisson equation to be satisfied at each order in this expansion. Clearly, the Boltzmann equation is not satisfied when going beyond the saddle point, and this is the reason for deviations from the Poisson-Boltzmann equation. Particularly useful is the introduction of the Gibbs potential $\Gamma[\psi]$, which only contains one-particle irreducible diagrams (and thus reduces the number of diagrams to be considered) and which allows to directly calculate the electrostatic potential distribution via the equation of state. We applied our formalism to the case of a charged wall which is impenetrable to counter ions and obtained, to one-loop order and without further approximations, the electrostatic potential, the counter-ion distribution, and the effective interactions between test particles. We find that the counter-ion density is increased close to the wall as compared to the mean-field (Poisson-Boltzmann, PB) solution, however, right at the wall the density is unchanged as compared to PB. The increase close to the wall is due to correlations between counter ions, which are not captured in the PB approach and which reduce the repulsion between counter ions. The surface potential is increased at the surface. The relative strength of the one-loop correction is proportional to the single parameter $\tilde{\ell}_B/4\pi\mu = 2\pi q^3 \ell_B^2 \sigma$ and thus is proportional to the cube of the counter ion valency. Our results become unphysical at $\tilde{\ell}_B/4\pi\mu \approx 12$. The value of $\tilde{\ell}_B/4\pi\mu$ up to which our results are accurate could only be inferred from quantitative comparisons with numerical simulations, which we plan to do in the future. Our formalism can in principle be applied to all situations where the PB equation can be solved in closed-form. It would be particularly useful to obtain the one-loop correction for a charged wall in a salt solution, because this would represent the bridge between Debye-Hückel and Poisson-Boltzmann theory.

-
- [1] G. Gouy, J. Phys. **9**, 457 (1910); Ann. Phys. **7**, 129 (1917).
 - [2] D.L. Chapman, Philos. Mag. **25**, 475 (1913).
 - [3] O. Stern, Z. Elektrochem. **30**, 508 (1924).
 - [4] R.M. Fuoss, A. Katchalsky, and S. Lifson, Proc. Natl. Acad. Sci. U.S.A. **37**, 579 (1951).
 - [5] D. Andelman, Ch. 12 in *Handbook of Biological Physics, Vol. 1*, R. Lipowsky and E. Sackmann, eds., (Elsevier, 1995).
 - [6] S. Levine and C.W. Outhwaite, J. Chem. Soc., Faraday Trans. 2 **74**, 1670 (1978); C.W. Outhwaite and L.B. Bhuiyan, *ibid.* **79**, 707 (1983).
 - [7] D. Henderson, L.Blum, and W.R. Smith, Chem. Phys. Lett. **63**, 381 (1979).
 - [8] P. Nielaba and F. Forstmann, Chem. Phys. Lett. **117**, 46 (1985); B. D’Aguanno, P. Nielaba, T. Alts, and F. Forstmann **85**, 3476 (1986); P. Nielaba, T. Alts, B. D’Aguanno, and F. Forstmann **34**, 1505 (1986).
 - [9] G.M. Torrie and J.P. Valleau, Chem. Phys. Lett. **65**, 343 (1979); J. Chem. Phys. **73**, 5807 (1980); J. Phys. Chem. **86**, 3251 (1982).
 - [10] W. van Meegen and I Snook, J. Chem. Phys. **73**, 4656 (1980).
 - [11] B. Svensson and B. Jönsson, Chem. Phys. Lett. **108**, 580 (1984).
 - [12] B. Svensson, B. Jönsson, and C.E. Woodward, J. Phys. Chem. **94**, 2105 (1990).

- [13] M. Lozada-Cassou, J. Chem. Phys. **80**, 3344 (1984).
- [14] R. Kjellander and S. Marčelja, Chem. Phys. Lett. **112**, 49 (1984); J. Chem. Phys. **82**, 2122 (1985).
- [15] R. Kjellander, T. Akesson, B. Jönsson, and S. Marčelja, J. Chem. Phys. **97**, 1424 (1992).
- [16] B. Jönsson, H. Wennerström, and B. Halle, J. Phys. Chem. **84**, 2179 (1980).
- [17] L. Guldbbrand, B. Jönsson, H. Wennerström, and P. Linse, J. Chem. Phys. **80**, 2221 (1984).
- [18] P. Attard, Adv. Chem. Phys. **XCII**, 1 (1996).
- [19] R. Podgornik and B. Zeks, J. Chem. Soc. Faraday Trans. 2 **84**, 611 (1988); R. Podgornik, J. Phys. A **23**, 275 (1990).
- [20] P. Attard, D.J. Mitchell, and B.W. Ninham, J. Chem. Phys. **88**, 4987 (1988); *ibid.* **89**, 4358 (1988).
- [21] J. Schwinger, Proc. Natl. Acad. Sci. **37**, 452 (1951); **37**, 455 (1951); **44**, 956 (1958).
- [22] E. Brézin, J.C. Le Guillou, and J. Zinn-Justin, in *Phase Transitions and Critical Phenomena*, Vol. VI, C. Domb and M.S. Green, eds. (Academic Press, N.Y., 1976).
- [23] *Handbook of Mathematical Functions*, M. Abramowitz and I.A. Stegun, eds. (Dover Publications, New York, 1972).
- [24] B. Jancovici, J. Stat. Phys. **28**, 43 (1982).
- [25] M. Baus, Mol. Phys. **48**, 347 (1983).
- [26] S.L. Carnie and D.Y. Chan, Mol. Phys. **51**, 1047 (1984).

FIG. 1. a) One-loop and b) two-loop diagrams that enter the calculation of the logarithm of the partition function, Eq.(18). The two-loop diagram to the right is one-particle reducible and thus cancels out when going to the Gibbs potential, Eq.(19).

FIG. 2. Plot of the rescaled self-energy g as a function of the rescaled distance from the wall, z/μ , as determined by Eq.(42). The asymptotic behavior for small and large wall distance, Eqs.(45) and (46), are drawn as broken lines in a) and b), respectively.

FIG. 3. Plot of the rescaled correction to the electrostatic potential f , as defined by Eq.(50). The asymptotic results for small and large separation from the wall, Eqs.(52) and (53), are denoted by broken lines.

FIG. 4. Plot of the rescaled one-loop correction to the counter ion density h , as defined by the Eqs.(60) and (61). One notes that the density change at the substrate surface vanishes identically.

FIG. 5. Plot of the one-loop prediction for the rescaled density $\bar{\rho}(z) = (\tilde{\ell}_B \mu^2 / 2) \rho(z)$ as a function of the rescaled distance from the wall z/μ , for four different values of the parameter $\tilde{\ell}_B / 4\pi\mu$. The broken line denotes the PB result; the other three solid lines are for $\tilde{\ell}_B / 4\pi\mu = 1, 5, \text{ and } 10$, with the distance to the PB curve increasing as $\tilde{\ell}_B / 4\pi\mu$ increases.

Figure1, Netz and Orland

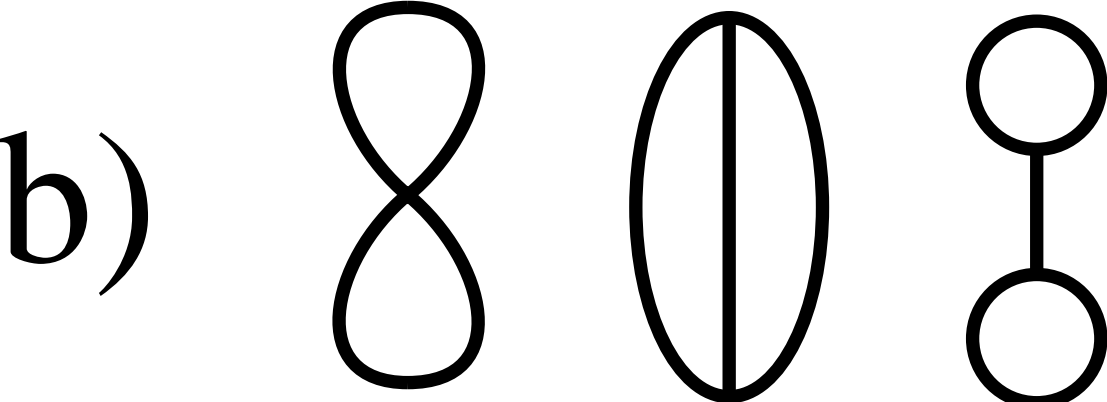
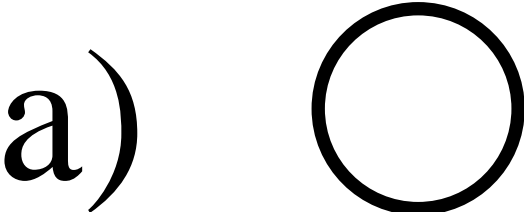


Fig.2a, Netz and Orland

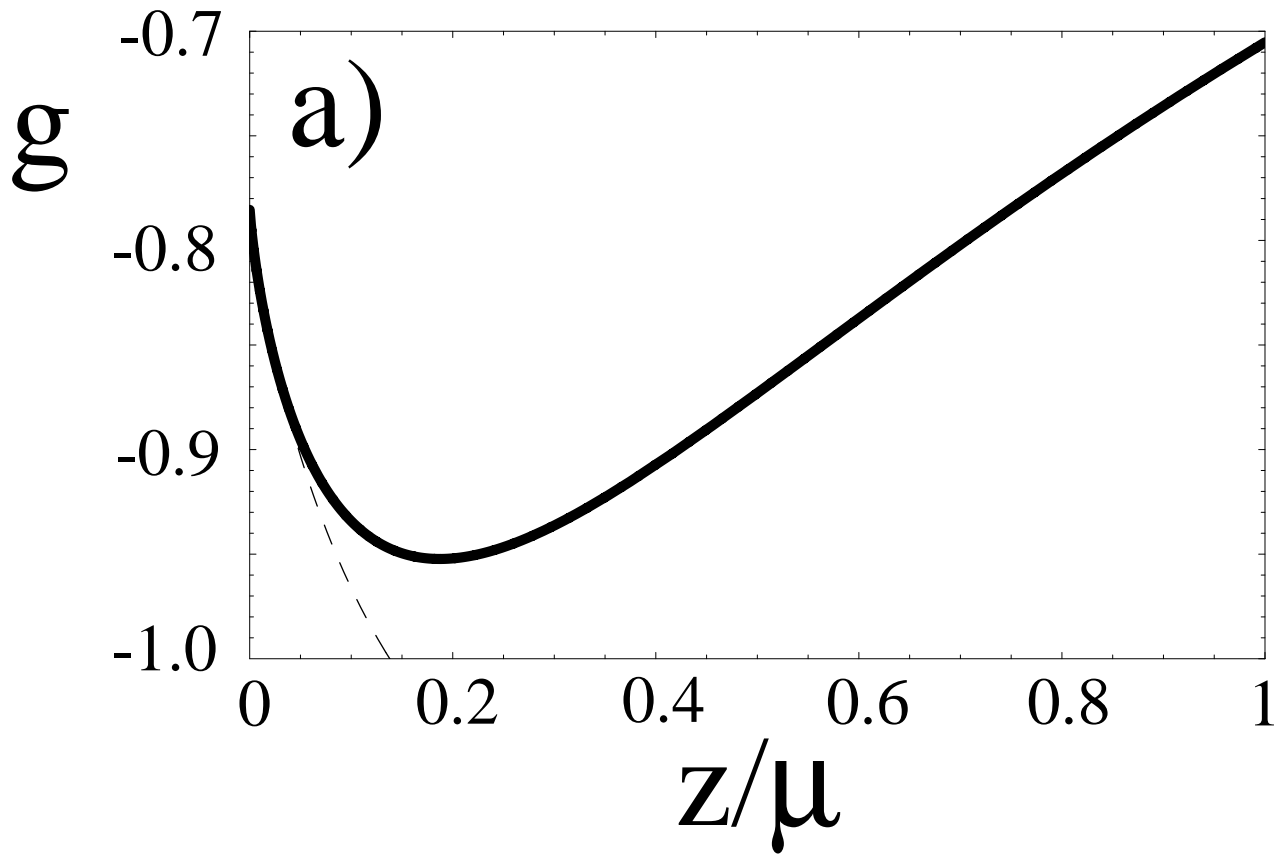


Fig.2b, Netz and Orland

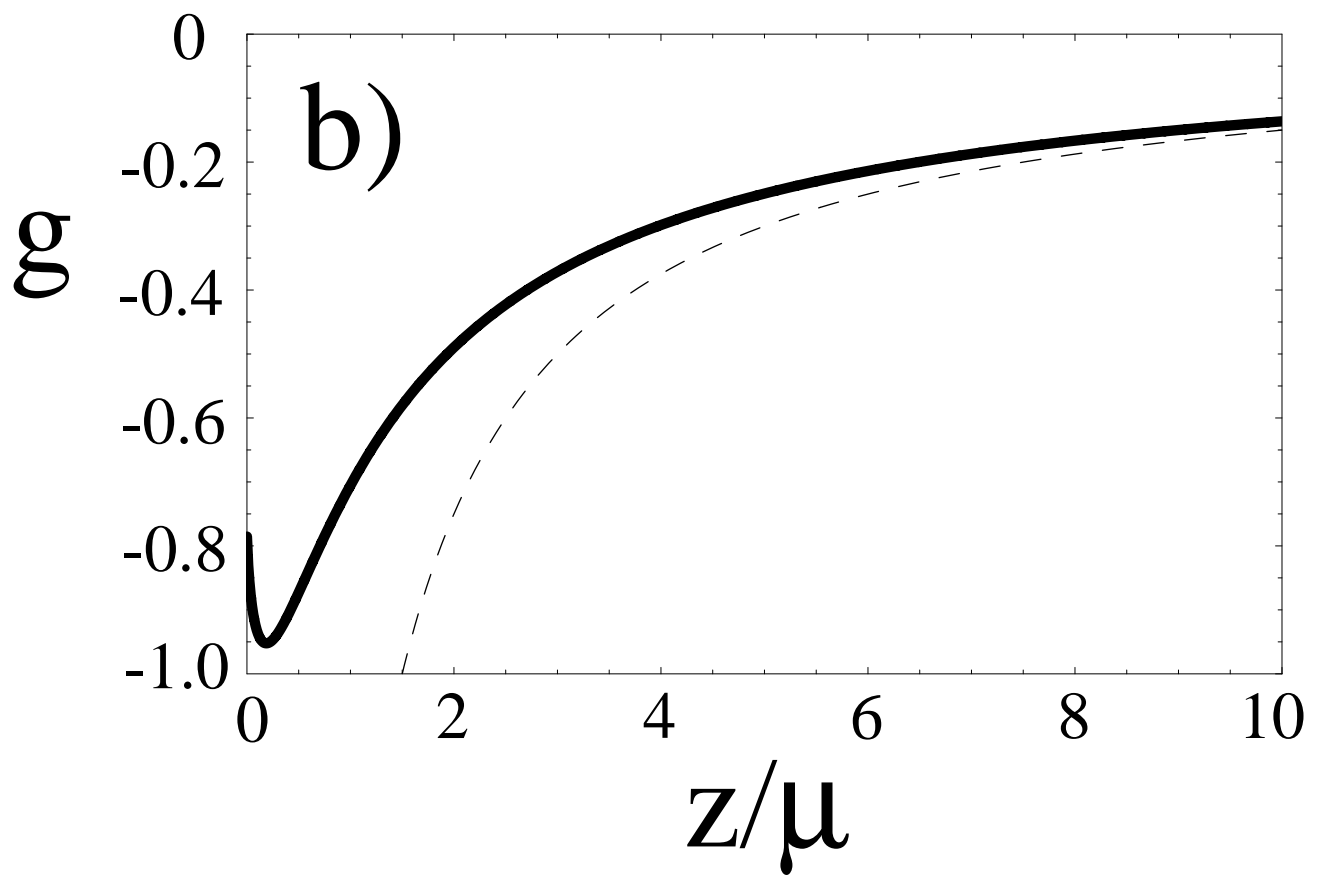


Fig.3a, Netz and Orland

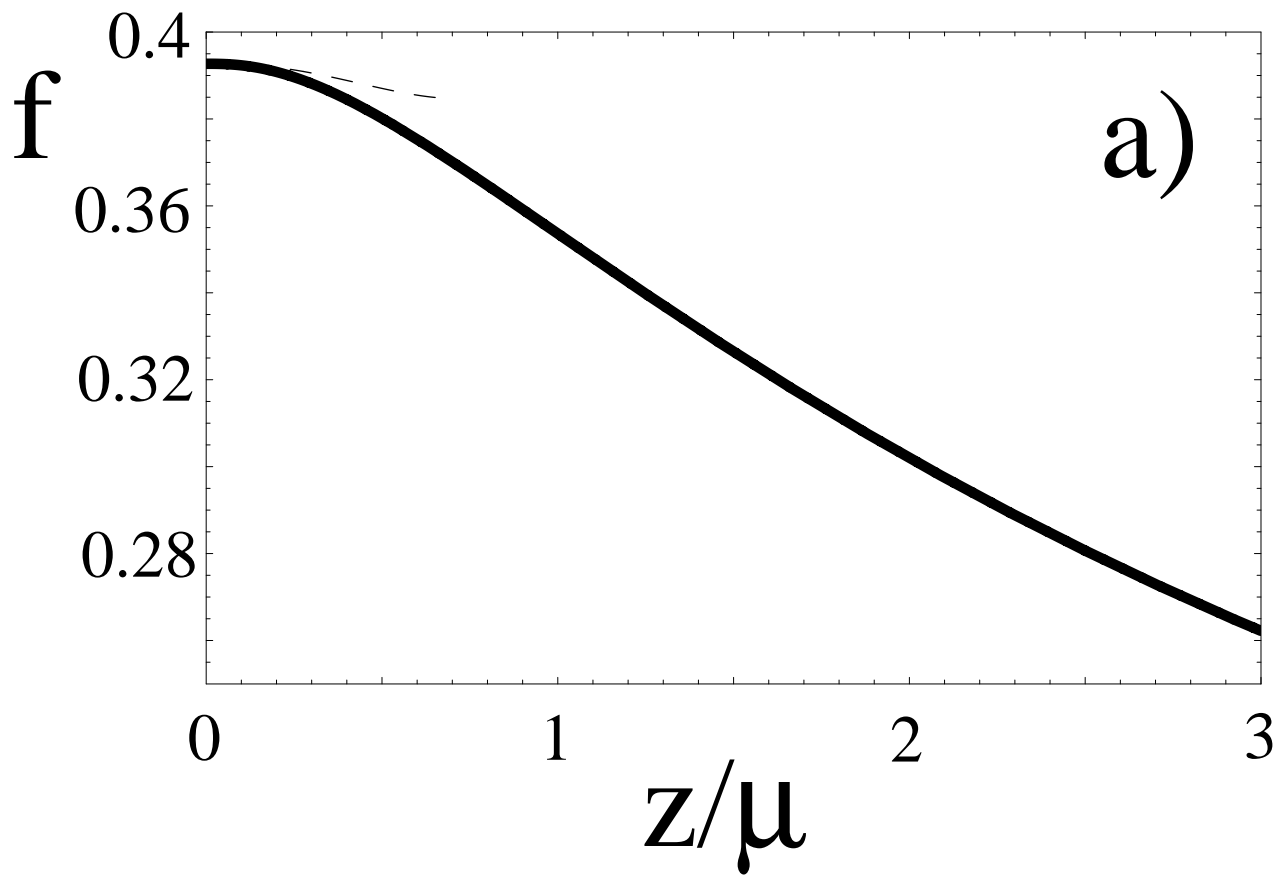


Fig.3b, Netz and Orland

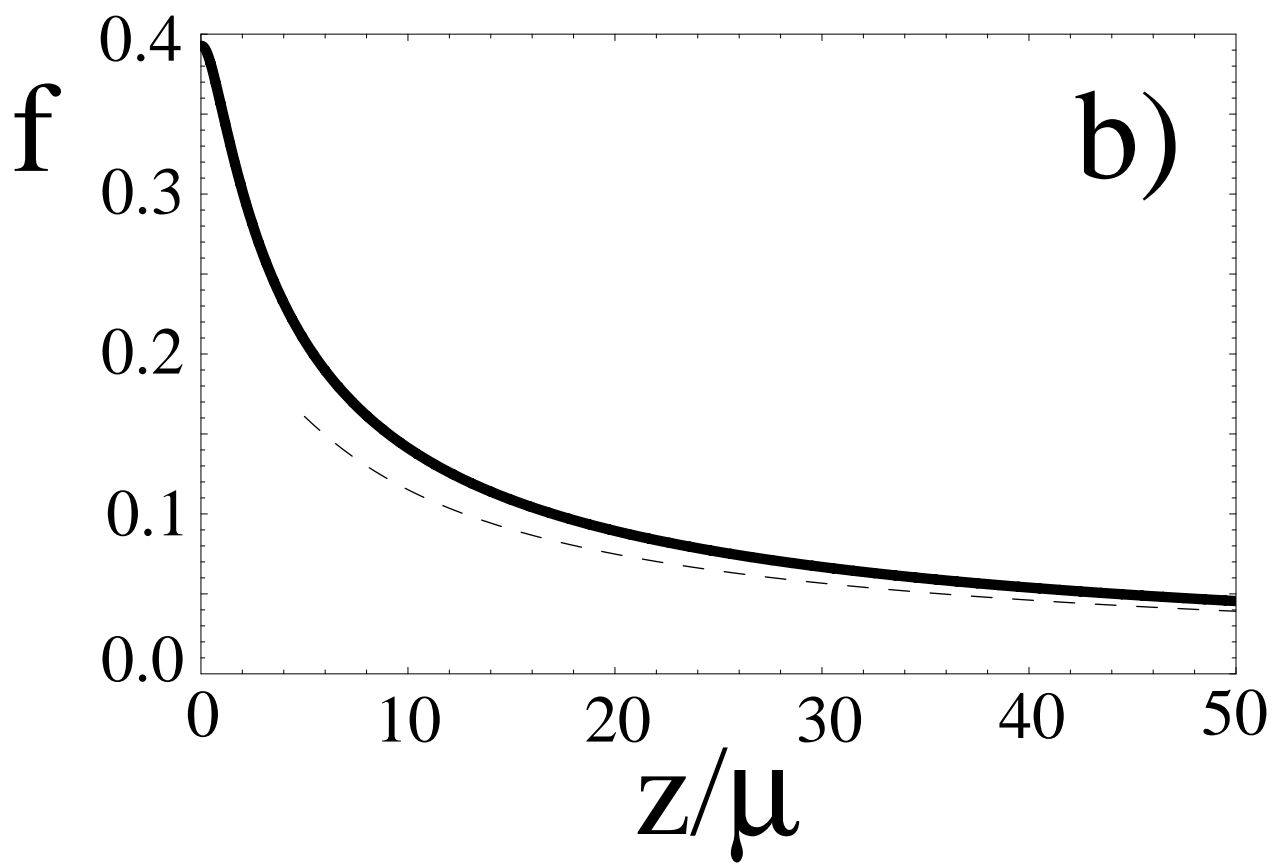


Fig.4a, Netz and Orland

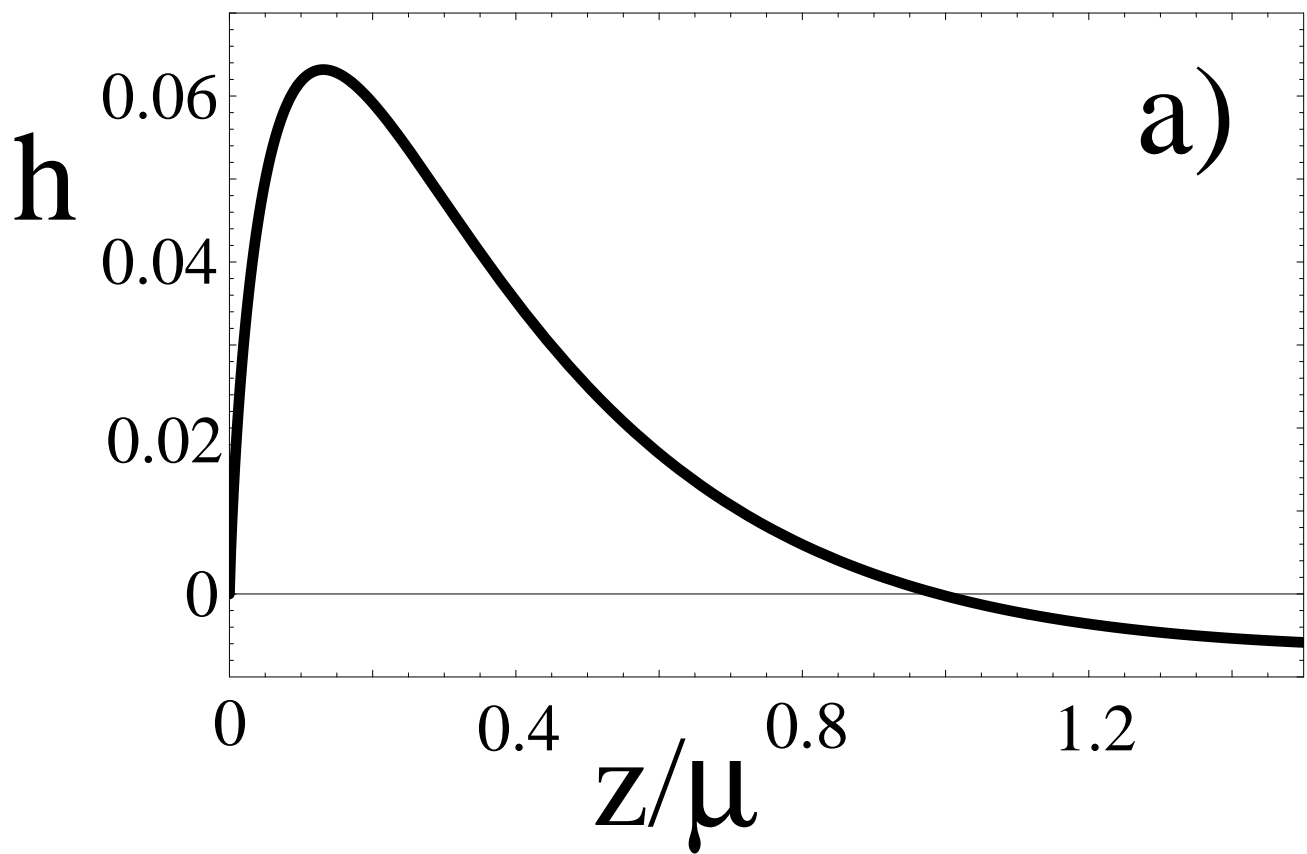


Fig.4b, Netz and Orland

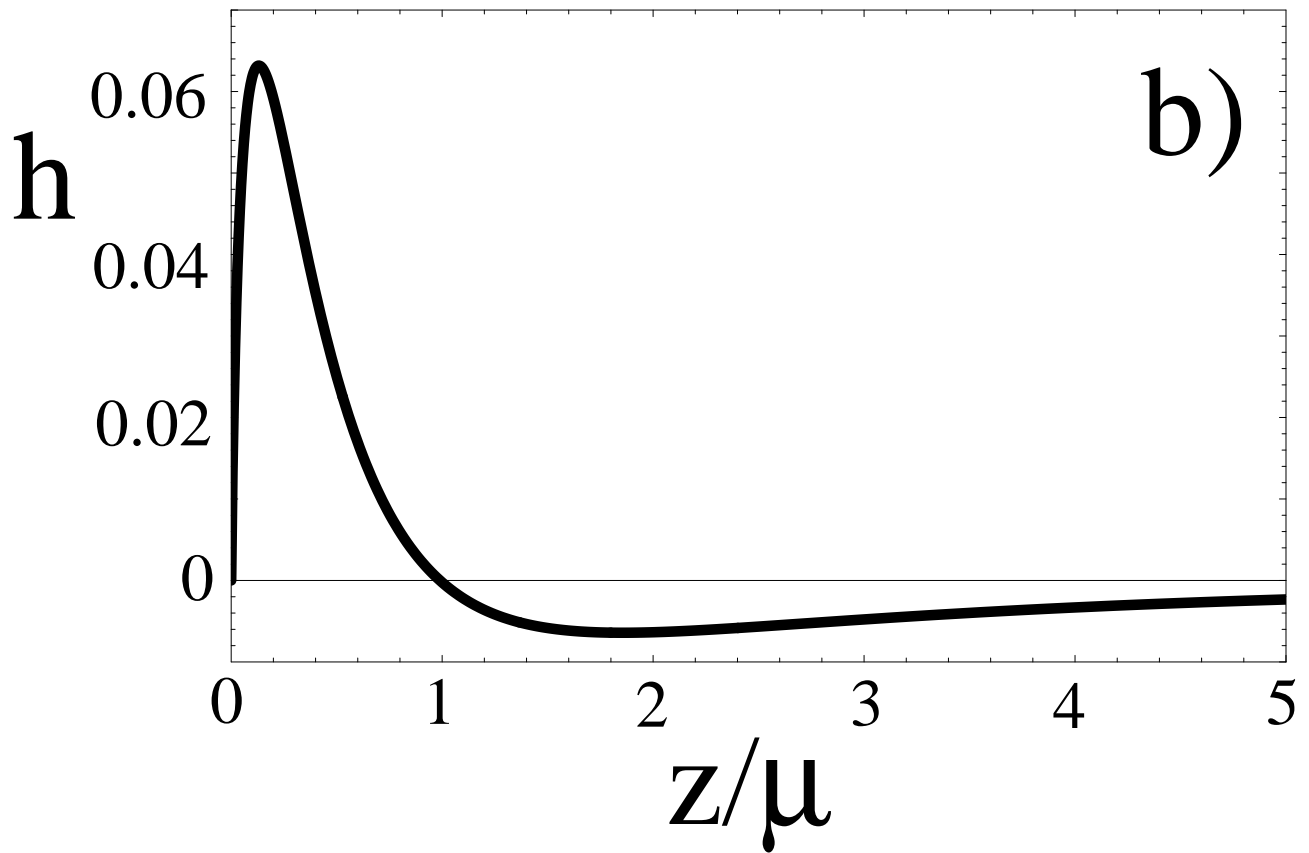


Fig.5, Netz and Orland

